Simplified hydrodynamic analysis on the general shape of the hill charts of Francis turbines using shroud-streamline modeling

IOP Conf. Series: Journal of Physics: Conf. Series **1042** (2018) 012003 doi:10.1088/1742-6596/1042/1/012003

Simplified hydrodynamic analysis on the general shape of the hill charts of Francis turbines using shroud-streamline modeling

I Iliev[1], C Trivedi[1] and O G Dahlhaug[1]

[1*]Waterpower Laboratory, Department of Energy and Process Engineering, Norwegian University of Science and Technology, NO-7491 Trondheim, Norway

E-mail: igor.iliev@ntnu.no

Abstract. The paper presents a simplified one-dimensional calculation of the efficiency hill-chart for Francis turbines, based on the velocity triangles at the inlet and outlet of the runner's blade. Calculation is done for one streamline, namely the shroud streamline in the meridional section, where an efficiency model is established and iteratively approximated in order to satisfy the Euler equation for turbomachines at a wide operating range around the best efficiency point (BEP). Using the presented method, hill charts are calculated for one splitter-bladed Francis turbine runner and one Reversible Pump-Turbine (RPT) runner operated in the turbine mode. Both turbines have similar and relatively low specific speeds of $n_{sQ} = 23.3$ and $n_{sQ} = 27$, equal inlet and outlet diameters and are designed to fit in the same turbine rig for laboratory measurements (i.e. spiral casing and draft tube are the same). Calculated hill charts are compared against performance data obtained experimentally from model tests according to IEC standards for both turbines. Good agreement between theoretical and experimental results is observed when comparing the shapes of the efficiency contours in the hill-charts. The simplified analysis identifies the design parameters that defines the general shape and inclination of the turbine's hill charts and, with some additional improvements in the loss models used, it can be used for quick assessment of the performance at off-design conditions during the design process of hydraulic turbines.

1. Introduction

Efficiency of hydraulic Francis turbines at off-design operating conditions is governed by the shapes of their performance hill-charts [1-3]. All parameters that define the wetted surfaces of a turbine passage, both rotating and stationary, has influence on the total efficiency at each operating point defined by the head, discharge and rotational speed of the runner [4]. Depending on the type and location, turbine losses can be typically classified into

- Spiral casing losses (due to skin friction and secondary flow);
- Stay and guide-vane losses (due to secondary flow, wake mixing, skin friction and incidence);
- Runner losses (due to flow incidence at inlet, skin friction in the blade channels, three-dimensional and curvature effects and residual swirl at the outlet);
- Draft tube losses (due to skin friction, flow in an elbow and channel divergence).

Not listed in the losses classification is the slip effect in the runner, which is mainly governed by the (1) relative whirl in the blade channel generated by the finite number of runner blades, and (2)

the energy distribution along the blade length. These effects are usually modelled with a slip factor that has indirect influence on the peak efficiency and the location of the BEP point in the hill-chart.

Experimental and numerical results have showed that runner and draft-tube losses can account for up to 50% of the total losses at best-efficiency point (BEP) [5-7]. Normally, runner and draft-tube losses will further increase to an even higher percentage when the turbine is being operated at off-design operating conditions, i.e. part-load (PL) and full load (FL). Considering the global parameters of the turbine, prior knowledge of the shape of the hill-chart can be obtained by conducting a single-streamline hydrodynamic performance analysis. Mean-streamline models are usually used for performance prediction in the design stage of both compressible and incompressible flow in runners and impellers of mixed-flow turbo machines [8-11]. The accuracy of these models, however, relies heavily on the needed coefficients that are rarely reported in the open literature.

On the other hand, Computational Fluid Dynamics (CFD) is a powerful tool that can predict the hill-charts with a high accuracy and is becoming more and more practical for automatically guided design and optimization of turbomachinery [12-14]. However, when analytical insight is needed in order to provide understanding of what drives the general shape of the turbine hill charts, CFD is usually not the way to go.

The focus in this paper is to examine the ability to predict the general shape of the hill-chart of a two low-specific-speed Francis turbines by only using simplified models for the runner losses based on the velocity triangles at the inlet and outlet of the shroud streamline. Since the only difference between the two examined turbines is in the runner design, it indicates that the differences in the general shapes of their hill charts (experimentally measured) could be linked with the losses in and downstream of their runners.

2. Specifications and description of the analyzed runners

Two low specific speed Francis turbine runners, which were available for model tests at the Waterpower laboratory, were used for the theoretical analysis of the general shape of their hill-charts. Both runners are designed to fit in the same test-rig, i.e. same distributor and draft-tube, but originate from different research activities in the aforementioned laboratory [15, 16]. Marked as "F99" is the splitter-bladed Francis turbine runner, while "RPT" represents the reversible pump-turbine runner (see figure 1 below). Global parameters that were used in the theoretical analysis are specified in table 1.

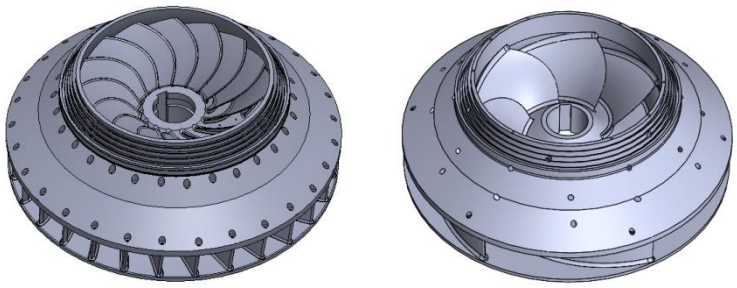

Figure 1. Comparison of the geometries for both runners.
F99 – on the left, RPT – on the right.

The F99 runner has 15 full-length blades and 15 splitter blades with a model peak efficiency of $\eta_h = 92.6\%$ when operated in an open loop under a net head of $H_n = 12\ [m]$. The RPT runner has 6 full-length blades with a model peak efficiency of $\eta_h = 89.6\%$ when operated in the same rig as the F99 model. The common distributor is comprised of 14 stay vanes and 28 guide vanes and the common draft-tube is an elbow type. Hence, the most effective difference between both runners is the reaction ratio ($R^{F99} = 0.533$ and $R^{RPT} = 0.789$) and the prescribed stream wise angle distribution along the blade's mid surface. The specific speeds of both runners are $n_{sQ} = 23.3$ and $n_{sQ} = 27$ in $[rpm\ m^{3/4}\ s^{-1/2}]$, for F99 and RPT respectively.

Table 1. Global parameters used as input for both runners

	F99		RPT	
Parameter	Inlet	Outlet	Inlet	Outlet
Diameter D [mm]	621.6	349	630.5	349
Runner width b [mm]	58.7	/	58.7	/
Blade angle β [deg]	63.38	19.62	12.02	13.45
Number of blades Z [-]	30	15	6	6
Blade length L_b [mm]	250		690	

Experimental data used for comparison is obtained from model tests done at the Waterpower Laboratory from different measuring campaigns. The test rig has the possibility to be operated in open and closed loop and according to the IEC 60193 standard for model tests [17].

3. Description of the solution procedure and modelling of the runner losses

The calculation of efficiency for the operating points used to construct the hill charts is done by modelling the incidence and residual swirl losses in the runner, as well as the friction losses in the runner and draft tube. These losses are modelled as a function of vector components from the inlet and outlet velocity triangles on the shroud streamline of the runner. Iterative procedure is than constructed using MATLAB in order to find the needed velocity triangles that will satisfy both the efficiency models and the Euler equation for each operating point. The Euler equation for hydraulic turbines, representing the hydrodynamic work exchanged between the fluid and the runner blades, is given by:

$$gH_n\eta_h = u_1c_{1u} - u_2c_{2u} \tag{1}$$

where indices 1, 2 denote the location at the inlet and outlet of the runner respectively, g – gravitational constant, H_n – net head, η_h - hydraulic efficiency, u – circumferential velocity at specific location, c_u – projection of the absolute velocity in the circumferential direction at specific location.

For a given rotational speed of the runner – ω and for given turbine discharge – Q, the components of the outlet velocity triangle can be calculated (see figure 2). The circumferential velocity c_{2u}, needed for the second term on the right hand side of equation (1), is calculated from the velocity triangle for infinite number of runner blades corrected by the approximated slip factor Δ_2 [18]:

$$|\overrightarrow{c_{2u}}| = \sqrt{c_2^2 - c_{2m}^2}; \qquad \overrightarrow{c_2} = \overrightarrow{u_2} + \overrightarrow{w_{2\infty}} + \overrightarrow{\Delta_2}; \qquad |\overrightarrow{\Delta_2}| \approx \frac{\pi u_2 \sin\beta_2}{Z_2}; \qquad c_{2m} = \frac{4Q}{\phi\pi D_2^2} \tag{2}$$

where c_{2m} – meridional component of the absolute velocity c, w_∞ - theoretical relative velocity in the rotating frame of reference for infinite number of blades, ϕ – blockage coefficient at the outlet of the runner due to the thickness and angle of the runner blades, usually in the range of 0.9-0.85 [18, 19]. In the present work, the upper limit value is used for the F99 while the lower limit value is used for the RPT.

At the inlet, calculation becomes a bit more complicated due to the fact that efficiency is unknown. The available hydraulic energy of the fluid ($E\eta_h = gH_n\eta_h$) will produce total circulation of $\Gamma_1 = \oint_l c_{1u}r_1 d\varphi = 2\pi r_1 c_{1u}$ at the inlet of the runner, which will, also from the Euler equation, result in:

$$c_{1u} = \frac{\Gamma_1}{2\pi r_1} = \frac{gH_n\eta_h + u_2c_{2u}}{u_1} \tag{3}$$

where $r_1 = D_1/2$. Again, due to the relative whirl that exists between the finite number of blades at the inlet of the runner, this velocity component will be corrected by the approximate slip factor calculated as:

$$\left|\overrightarrow{\Delta_1}\right| \approx \frac{\pi u_1 \sin\beta_1}{z_1}; \qquad \overrightarrow{c_1} = \overrightarrow{u_1} + \overrightarrow{w_{1\infty}} + \overrightarrow{\Delta_1}; \tag{4}$$

Hence, even for the BEP point, this will result in a misalignment, between the blade angle at the runner inlet and the fluid flow angle, which can be reduced by increasing the number of runner blades, by reduction of circumferential velocity or by decreasing the blade angle.

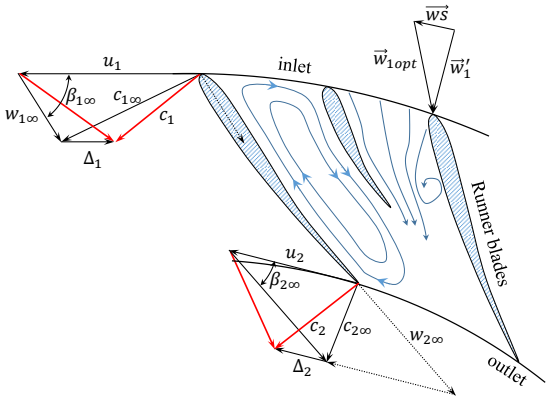

Figure 2. Illustration of velocity triangles for finite and infinite number of blades

Together with equation 3, another equation is needed for the calculation of efficiency. Simple efficiency models for the losses in the runner and draft tube are introduced hereafter.

Incidence loss at the inlet of the runner

Incidence loss is caused by the difference between the direction of the fluid flow and the fixed blade angle at the inlet of the runner (see figure 2). The fluid that is about to enter the runner will have a relative velocity $\vec{w}_1'$ that is a function of the rotational speed ω, available energy $E\eta_h$ and the discharge Q, while the fluid that has already entered the runner will quickly align to and follow the surfaces of the runner blades (i.e. relative velocity at optimum incidence $\vec{w}_{1opt}$). Assuming that the vector difference between the relative fluid velocity and the optimum incidence for the same discharge is lost ($\overrightarrow{ws} = \vec{w}_1' - \vec{w}_{1opt}$), a simplified incidence loss model can be established by writing [10]:

$$\Delta\eta_{incidence} = \frac{|\overrightarrow{ws}|^2}{2gH_n} \tag{5}$$

Swirl loss at the outlet of the runner

Swirl loss is a kinetic energy loss due to the residual whirl being created at the outlet of the runner from the mismatch of the rotational speed to the turbine discharge. The draft tube is than unable to transform this kinetic energy into pressure and this energy is lost in the lower reservoir. Depending on the type of draft tube and its stream wise increase of the draft tube cross section area, free-vortex-flow effect will reduce this kinetic energy before the fluid leaves the draft tube [1]. Nevertheless, assuming that 90% of the whirling kinetic energy at runner outlet is lost, a simplified swirl loss model can be established as:

$$\Delta\eta_{swirl} = 0.9 \cdot \frac{c_{2u}^2}{2gH_n} \tag{6}$$

Friction loss between runner blades

Friction loss in the blade channel of the runner is due to the shear forces in the boundary layers attached to the wetted surfaces. In analogy with the friction factor for calculation of pipe losses, using the average of the squared relative velocity at the inlet and outlet of the runner $\overline{w}^2 = (w_1^2 + w_2^2)/2$,

and the average hydraulic diameter between the inlet and the outlet of the blade channel $\bar{D}_h = (D_{h1} + D_{h2})/2$, a simplified model may be determined as:

$$\Delta\eta_{runner\_fric} = c_f \frac{L_b}{\bar{D}_h} \frac{\bar{w}^2}{2gH_n} \tag{7}$$

where c_f – skin friction coefficient. For the analysis in this paper, a constant value of the skin friction coefficient was assumed for both runners $c_f = 0.015$.

Friction and diffuser losses in the draft tube

Due to skin friction, secondary flow in the elbow and decelerating flow in the draft tube, pressure recovery will be done with some losses. For best elbow draft tubes installed in vertical turbines, Raabe [1] suggests using of the following model:

$$\Delta\eta_{DT} = 0.12 \frac{c_{2m}^2}{2gH_n} \tag{8}$$

Finally, combining all aforementioned losses yields the simplified loss model in the runner that is also used to model the total hydraulic efficiency in the Euler equation. This will introduce error in the results because total efficiency should include distributor losses, leakage losses, mixing losses, blade loading losses, disk friction losses, recirculation losses etc. However, for operation close to the BEP and in case of only examining the general shape of the hill chart, this simplified analysis should give a first clue on the expected performance of the runner and make an educated guess in case of a thorough optimization of the turbine.

$$\eta_h \approx 1 - \Delta\eta_{incidence} - \Delta\eta_{swirl} - \Delta\eta_{runner\_fric} - \Delta\eta_{DT} \tag{9}$$

The solution of the system of two equations (3) and (9) will give the values of circumferential component of the absolute velocity at the inlet of the runner c_{1u}, the hydraulic efficiency η_h and the angle of the fluid stream before entering the runner $\alpha_{1,in}$ (this angle should not be confused with the guide-vane opening angle α_{GV}), for each combination of the rotational speed of the runner – ω and the turbine discharge – Q. Net head H_n is assumed to be constant in the full range of the hill chart. Substitution of equation (9) into (3) will result into a transcendental equation that contains trigonometric functions of the dependent variable, requiring a special mathematical treatment that makes it difficult or most often impossible to solve analytically. Hence, an iterative procedure was employed to approximate the solution for each combination of ω and Q. The iteration procedure turned out to be extremely stable and, in order to achieve a rather remarkable convergence criteria of 10^{-9}, it requires only 20-40 iterations at each operating point and less than 5 seconds to compute the full hill chart, making it perfect for fast full-factorial optimization of the global parameters of the turbine [10].

4. Results and discussion

The calculation method described in section 3 was used to calculate a rather broad range of operating conditions for the two runners described in section 2. Side by side comparison of the measured and calculated hill chart for the F99 runner is given in figure 4, while the same is done for the RPT runner in figures 5 and 6. Regarding the general shape and the trend of the hill charts in figure 3, similarities can be observed with a close agreement for the position of the BEP. Also, for the theoretical calculation, the characteristic curves of zero incidence and zero swirl were precisely located and plotted on the right hand side hill chart. The zero swirl curve has a relatively low curvature for both runners and it passes through the origin of the $Q_{ED} - n_{ED}$ coordinate system. The slope of the zero incidence and zero swirl curves at the intersection point is governed by the geometry of the runner blades at the inlet and outlet respectively. Moving away from those two curves in the hill chart will increase the respective losses, and this effect, combined with the friction and draft tube losses at each point in the hill chart will yield the general shape of the efficiency isocurves. Single losses predicted for the F99 runner are presented on figure 3 for the four main losses modeled and used in equation (9). The arrows represent the direction of loss increase.

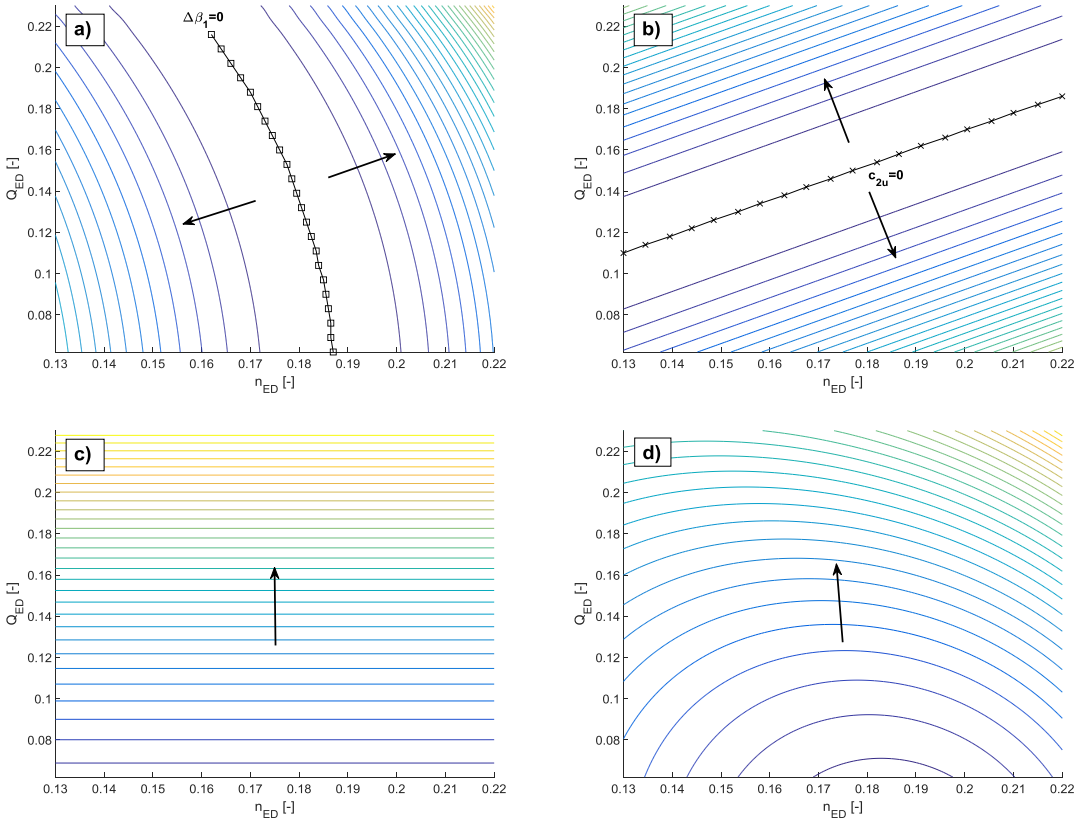

Figure 3. Efficiency decomposition into the four main losses for the F99 runner, with the arrow showing the direction of loss increase. a) contours of incidence losses, b) contours of swirl losses, c) contours of draft tube losses, d) contours of runner friction losses.

Comparing the curves of constant guide vane openings (measured) and constant flow angle at the inlet of the runner for the F99 (predicted), a significant difference can be seen for their locations in the hill chart area, with similar negative slope along the curves. This can be explained by (1) the expected nonlinear relation $\alpha_{GV}(\alpha_{1,i})$ and, (2) the losses in the circular cascade of guide vanes were not included in the analysis. If this was included in the calculation, despite the correction of the constant guide vane opening lines, prediction of absolute values of efficiency will also improve, especially in the zones away from the BEP.

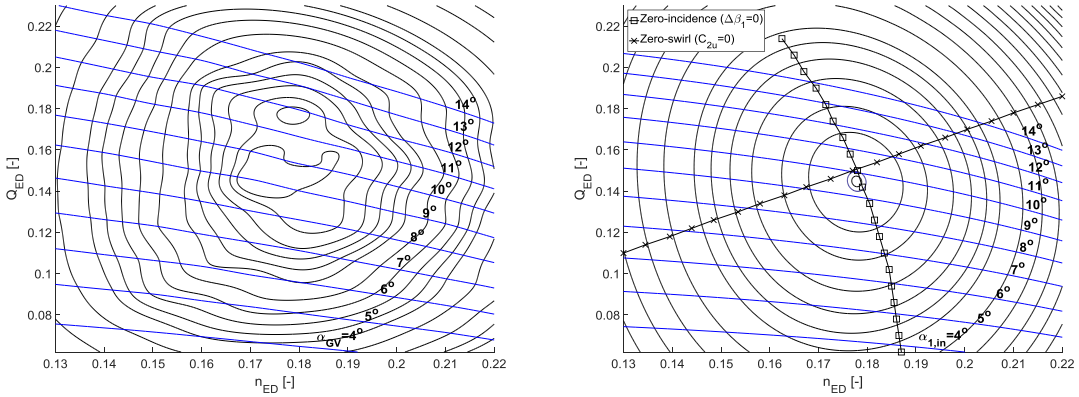

Figure 4. Hill charts of efficiency for the F99 runner.
Left side – measurements, right side – theoretical calculation

When comparing the result for the RPT runner shown on figure 5, a larger difference between measurements and theoretical calculation are observed. Comparable agreement for the general shape of the hill charts can be observed only on the right half of both hill charts (for n_{ED} larger than 0.22), while for the left half there is almost no agreement at all. The efficiency isocurves of the RPT are stretched in one direction that has a positive slope with reference to the n_{ED} axis. After careful examination of the possible reasons for the observed difference and comparing the measured data with data from previous measurements on the same models, it was concluded that the RPT runner is unexpectedly more sensitive to the Reynolds number than the F99 runner. Namely, the model test data used for this paper was obtained for open loop configuration of the test rig and at head $H_n \approx 12\ [m]$, resulting in Reynolds numbers ($Re = u_2 D_2/\nu$) lower than $2 \cdot 10^6$ for the left half of the graph, and lower than $3 \cdot 10^6$ for the entire range. This is well below the recommended value of $Re_{min} \geq 4 \cdot 10^6$ in the IEC standard [17].

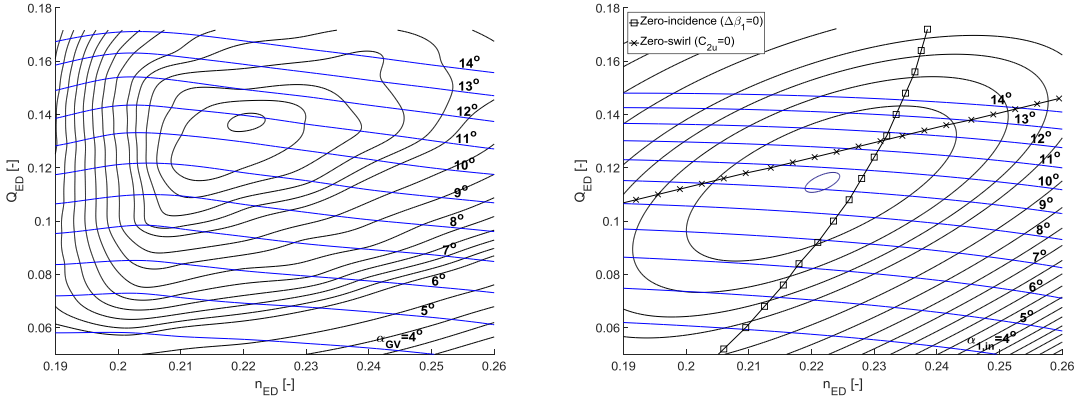

Figure 5. Hill charts of efficiency for the RPT runner.
Left side – measurements, right side – theoretical calculation

Efficiency measurements in a closed loop on the RPT model and for heads $H_n > 20\ [m]$ were previously reported by Olimstad [15]. These results are presented in figure 6, where the improvement in the Reynolds number effect is clearly visible for the left half of the hill chart previously mentioned. Additionally, the general shapes of the hill charts are more comparable to the theoretical calculation than previously seen in figure 5.

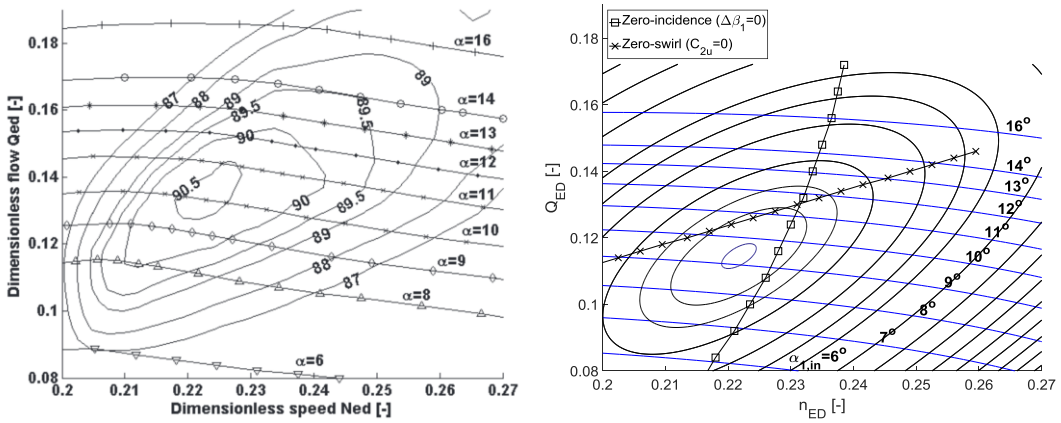

Figure 6. Hill charts of efficiency for the RPT runner.
Left side – measurements [15], right side – theoretical calculation

In the theoretical calculation, the position of the BEP is predicted to be at a lower Q_{ED} value when compared to the experimental results, while the n_{ED} value is pretty close in both cases. Similarly as for the F99 runner, there is an expected difference in the position of the curves of constant α_{GV} and $\alpha_{1,in}$ with a similar negative slope along the curves.

5. Conclusions

The theoretical analysis for the general shape of the hill chart presented here gives promising results using minimal geometric information for the turbine as the input. The turbine models selected for the analysis represent a rather special and interesting case since the only difference is the blade geometry of the runner, which nevertheless, gave large differences in the measured hill charts. The models used for predicting the losses in the runner and draft tube are extremely simple and intuitive and yet this was enough to give a comparable prediction for the hill chart shape of both runners and have provided a better understanding on which parameters are responsible for it.

The geometry of the shroud profile of the blade was used to simplify the complex three dimensional geometry of the runner where velocity triangles at the inlet and outlet of the runner were sought to satisfy the system of the Euler equation and the efficiency model. The numerical method used is also simple and stable, providing calculation of the full hill chart in less than 5 seconds. Based on the presented calculation and side-by-side comparison with experimental results, it was demonstrated that the shape of the hill charts is greatly dependent and driven by the geometry at the inlet and the outlet of the runner, namely the channel width, runner diameter and blade angle at the inlet and runner diameter and blade angle at the outlet. This is also characterized by the position and shape of the zero-incidence and zero-swirl curves in the hill charts, representing the joint hydrodynamic contribution from the inlet and outlet geometry of the runner.

The observed difference between absolute values of efficiency and guide vane opening at different operating conditions is expected and strongly dependent on the sophistication of the loss models used. Results can always be improved if more accurate models are used and more loss sources are simultaneously analyzed, such as the losses in the guide and stay vanes, blade loading losses, recirculation losses, disk friction and clearance gap leakages, etc. For prediction of the constant guide vanes opening curves, geometric relations and loss model is also needed. Using the free vortex flow and the radius of the trailing edge for the guide vanes, calculated values of $\alpha_{1,in}$ can be extrapolated and used as an input for such model.

6. References

[1] Joachim R 1985 Hydropower – the design, use, and function of hydromechanical, hydraulic, and electrical equipment *VDI Verlag*
[2] Grigori I K 1994 Hydraulic machines: turbines and pumps (Translated from Russian) *Lewis Publishers*
[3] Emil F M 1991 Water power development *Akademiai Kiado*
[4] Xin L, Yongyao L, Bryan W K, Weizheng W 2015 A selected literature review of efficiency improvements in hydraulic turbines *Renewable and Sustainable Energy Reviews* **51** 18-28
[5] Jurgen S, Helmut B, Helmut J 2016 Analysis of the Leakage Behaviour of Francis Turbines and Its Impact on the Hydraulic Efficiency - A Validation of an Analytical Model Based on Computational Fluid Dynamics Results *ASME. J. Fluids Eng.* **139(2)** 021106 (11 pages)
[6] Osterwalder J, Hippe L 2010 Guidelines for efficiency scaling process of hydraulic turbo machines with different technical roughness of flow passages *Journal of Hydraulic Research* **22:2** 77- 102
[7] Hermod B 1996 Analysis of losses in hydraulic turbines *Proceedings of the 18th IAHR symposium* 294-303
[8] Aungier R H 1995 Mean streamline aerodynamic performance analysis of centrifugal compressors *ASME J. of Turbomachinery* **117** 360-366

[9] Oh H W, Kim K Y 2001 Conceptual design optimization of mixed-flow pump impellers using mean streamline analysis *Proc. Instn. Mech. Engrs* **215** 133-138
[10] Pei-Yuan L, Chu-Wei G, Yin S 2015 A new optimization method for centrifugal compressors based on 1D calculation and analysis *Energies* **8** 4317-4334
[11] Galvas M R 1972 Analytical correlation of centrifugal compressor design geometry for maximum efficiency with specific speed *NASA TN **D-6729*** 1-42
[12] Risberg S, Jonassen M, Jonassen R 2008 Design of Francis turbine runners based on a surrogate model approach *The International Journal of Hydropower and Dams* **15(5)** 80-84
[13] Demeulenaere A, Ligout A, Hirsch C 2004 Application of multipoint optimization to the design of turbomachinery blades *Proc. of ASME Expo: Power for Land, Sea and Air* **5** 1481-1489
[14] Semenova A, Chirkov D, Lyutov A, Cherny S, Skorospelov V, Pylev I 2014 Multi-objective shape optimization of runner blade for Kaplan turbine *IOP Conf. Ser.: Earth Environ. Sci.* **22** 012025
[15] Grunde O, Torbjorn K N 2012 Stability limits of reversible-pump turbines in turbine mode of operation and measurements of unstable characteristics *ASME Fluids Eng.* **134** 111202
[16] Chirag T, Michel J C, Gandhi B K, Ole G D 2013 Experimental and numerical studies for a high head Francis turbine at several operating points *ASME Fluids Eng.* **135(11)** 111102
[17] IEC-60193, Hydraulic Turbines, Storage Pumps and Pump-turbines: Model Acceptance Tests, International standard, *International Electro-technical Commission*, 3, CH-1211 Geneva, Switzerland, 16 November, p. 578, 1999
[18] Geroff V 1973 Water turbines (In Bulgarian) *D. I. „Tehnika" Sofia*
[19] Stepanoff A J 1948 Centrifugal and axial flow pumps. Theory, design and application. *John Willey & Sons, Inc.*